

Supporting Information for: Engineering Bicontinuous Cubic Structures at the Nanoscale – the Role of Chain Splay

Chandrashekhar V. Kulkarni¹, Tsing-Young Tang², Annela M. Seddon^{1,3}, John

M. Seddon¹, Oscar Ces¹ and Richard H. Templer^{1*}

¹*Chemical Biology Centre, Department of Chemistry; ²Department of Chemistry, Imperial College, Exhibition Road, South Kensington, London, SW7 2AZ, UK; ³H.H.Wills Physics Laboratory, Tyndall Avenue, University of Bristol, Bristol BS8 1TL, UK*

1. Experimental Methods:

a) Sample Preparation

Our data were taken at increasing hydrations of 1-2 weight% and at temperature intervals of 5°C, using small and wide angle x-ray scattering. To prepare samples of fixed water composition, known amounts of lyophilized Monoelaidin (ME) or Monolinolein (ML) (Larodan Fine Chemicals AB, Sweden) were mixed with HPLC-grade water (Sigma-Aldrich Co.) directly into a 1.5mm diameter special glass X-Ray capillary (Gulmay Medical Ltd., UK). Samples were then centrifuged and subjected to a minimum of 10 freeze-thaw cycles crossing the chain melting temperature. Samples were subsequently equilibrated for 5-6 hours at room temperature. The capillaries were then flame sealed before a silicon sealant plug (Dow Corning Corp., USA) was applied. The samples were then subject to a further 10 freeze-thaw-centrifuge cycles. The weight of the sealed capillary before and after each temperature scan was noted.

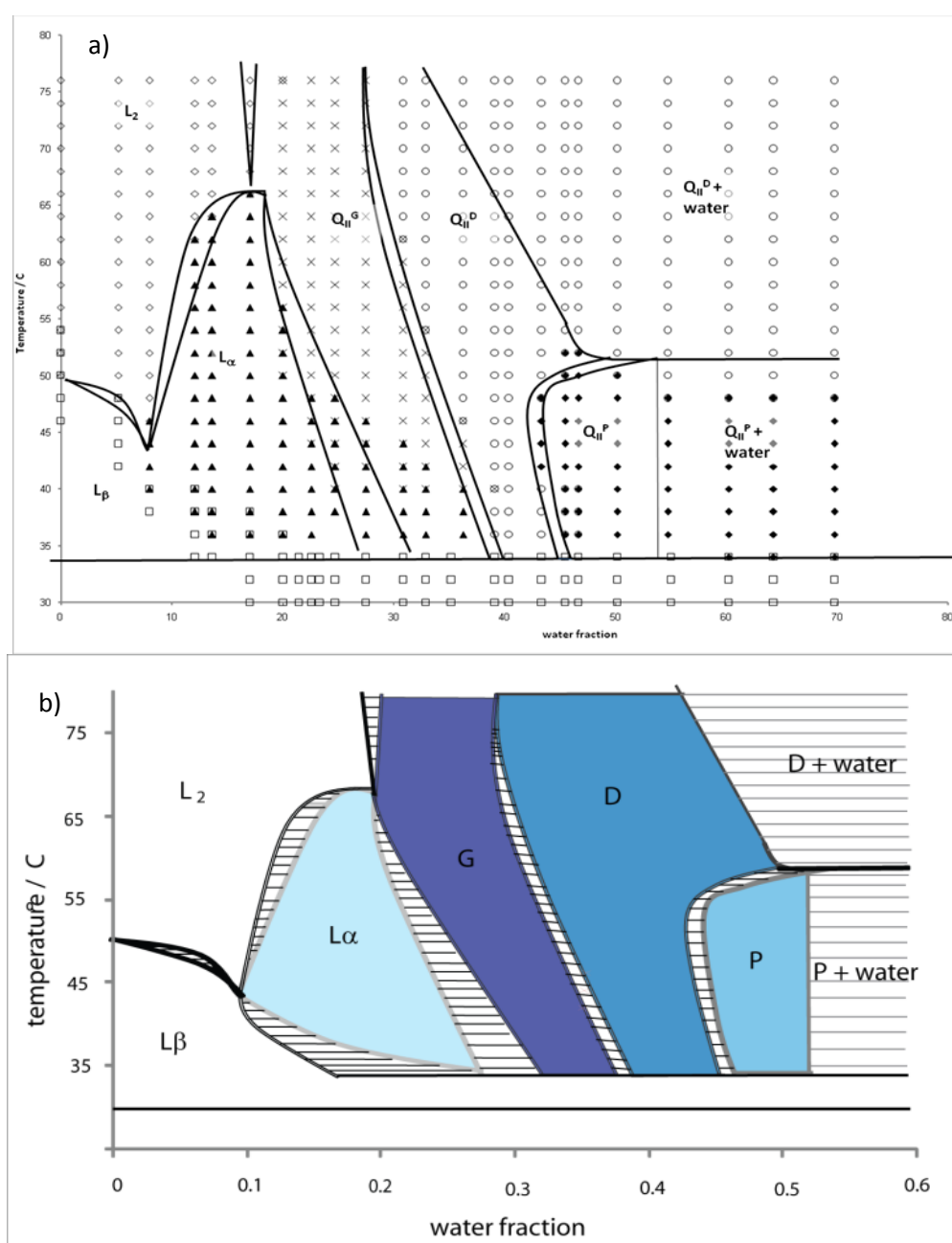
b) X-ray instrumentation

Low and wide angle X-ray diffraction patterns were obtained using two custom built X-ray beamlines. One is based around a microfocus source (Bede MicrosourceTM, Bede, UK)¹. A low divergence X-ray beam (2mrad) was created by using monolithic polycapillary optics (X-ray Optical Systems, Inc., USA). A Gemstar HS intensified charge coupled detector (Photonic Science Ltd, UK) was used to record the diffraction patterns. The detector-PC interface used a digital LVDS (RS-644) Picasso PCI-LS frame grabber card (ARVOO Imaging Products, Netherlands). Sample capillaries were located in a custom designed copper sample holder with Peltier driven temperature control (Melcor, USA). This provided temperature control to a precision of ± 0.05 °C and to an accuracy of ± 0.1 °C. The second beamline has X-rays generated by a FR591 rotating anode generator (Enraf-Nonius, Netherlands) running at 40kV and 30mA and focused using Franks Optics. Diffraction patterns were detected by an image intensified Charge Coupled device (CCD) camera (Photonic Science Ltd, UK). The capillaries were held in a custom built brass sample holder with Peltier driven temperature control via a Scorpion microcontroller (MicroRobotics, Cambridge, UK) accurate to 0.2°C and in a range from -20°C to 70°C. In both cases, heating scans were recorded between 30 and 75°C in increments of 2°C with equilibration times of 10 minutes at each temperature. The typical exposure time for a single image was between 15 and 30 seconds. A minimum of five images were collected per data point and summed prior to image analysis. Diffraction patterns were analyzed using an in-house developed software package, AXcess, using IDL language (ITT Visual Information Solutions, USA)². Lattice parameter values (in Å) were calibrated with silver behenate ($d_{001} = 58.38$ Å).

2. Construction of Phase Diagrams for ME and ML

The method by which the phase diagrams for ME and ML are constructed has been discussed in detail previously.³

Figure S1a) shows the raw data collected by SAXS and WAXS as described above used in the construction of the temperature – composition phase diagram for ME. Figure S1b) shows the phase diagram constructed from these data points. Figures S1c) and d) show the raw data used in the construction of the phase diagram for ML alongside the final phase diagram for ML respectively. The excess water boundaries were calculated from the positions where the lattice spacing for a given phase was found to remain constant upon the introduction of additional water.



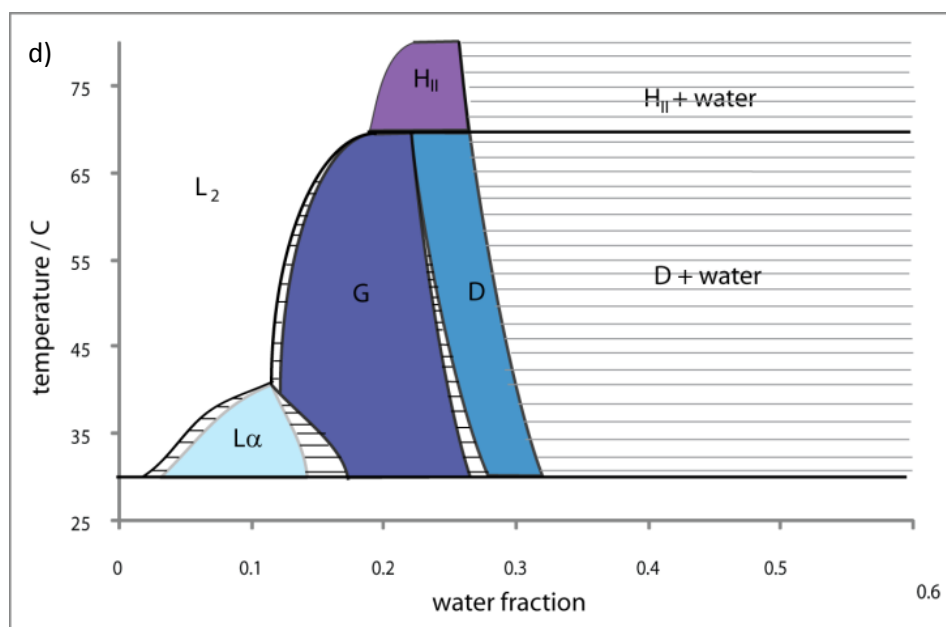
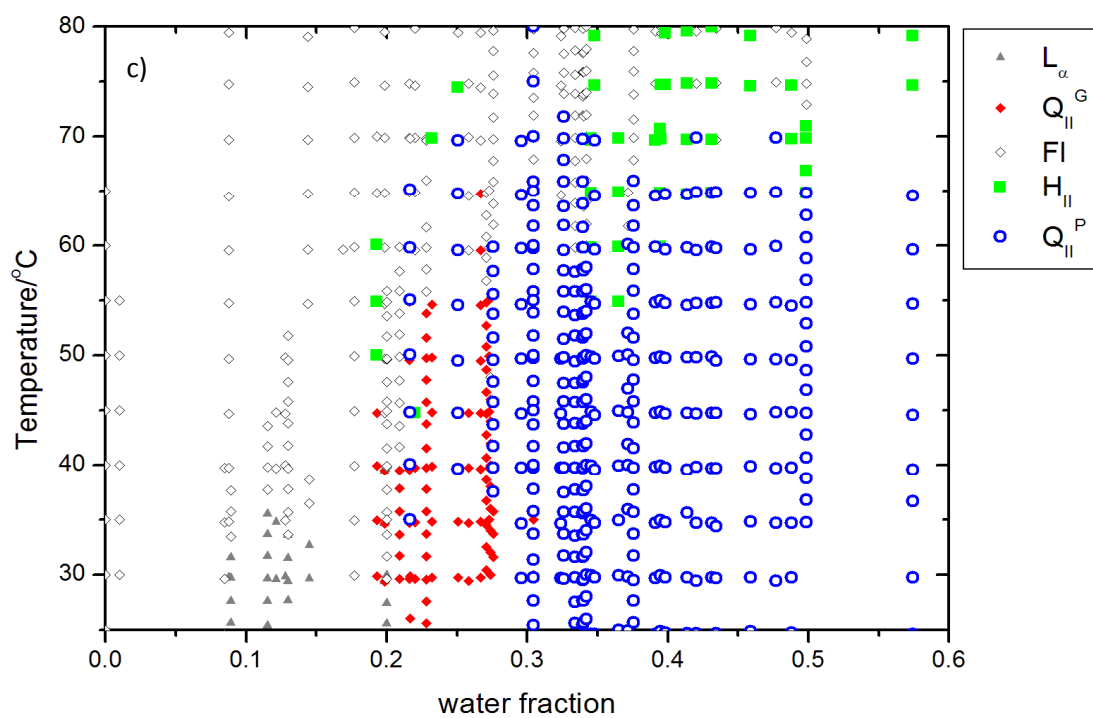


Figure S1: a) Raw data points collected by SAXS and WAXS used in the construction of the temperature composition phase diagram of ME; b) the resulting temperature composition phase diagram for ME; c) Raw data points collected by SAXS and WAXS used in the construction of the temperature composition phase diagram of ML; b) the resulting temperature composition phase diagram for ML.

Figures S2a) and b) show the experimental diffractograms, presented as stackplots generated by the in-house software AXcess² to highlight phase transitions for selected compositions of ME in water. Figures S2c) and d) show the corresponding data for ML.

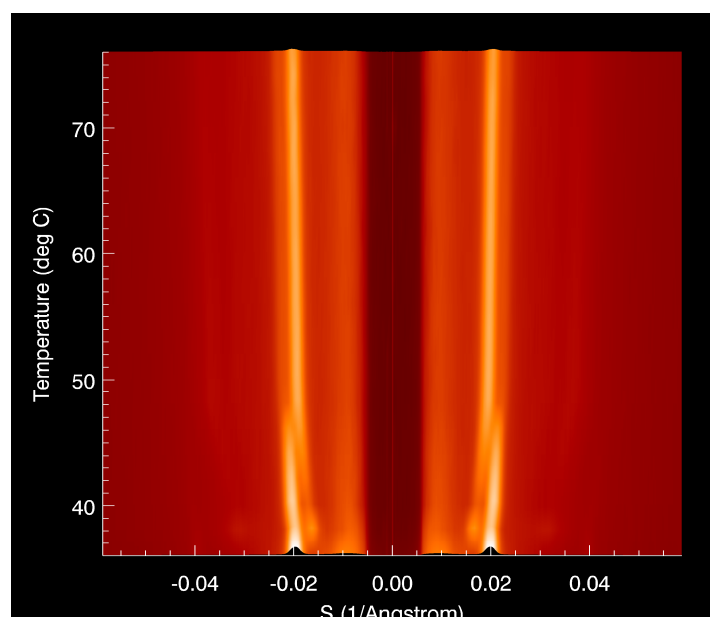


Figure S2a) Stackplot of diffractograms for ME in 24.72% water taken between 36 and 76°C showing the transition from $(L\beta) \rightarrow L\alpha \rightarrow L\alpha+G \rightarrow G$.

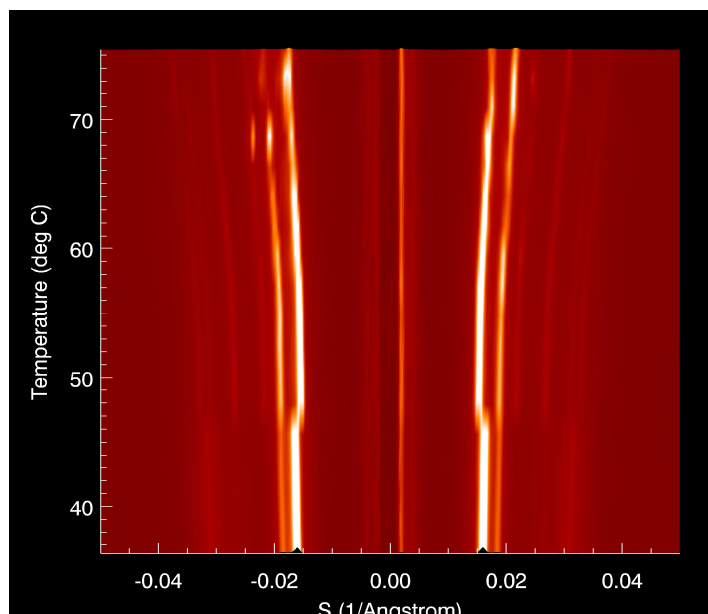


Figure S2b) Stackplot of diffractograms for ME in 35.55% water taken between 35 and 75°C at 2°C intervals showing the transition from G →D.

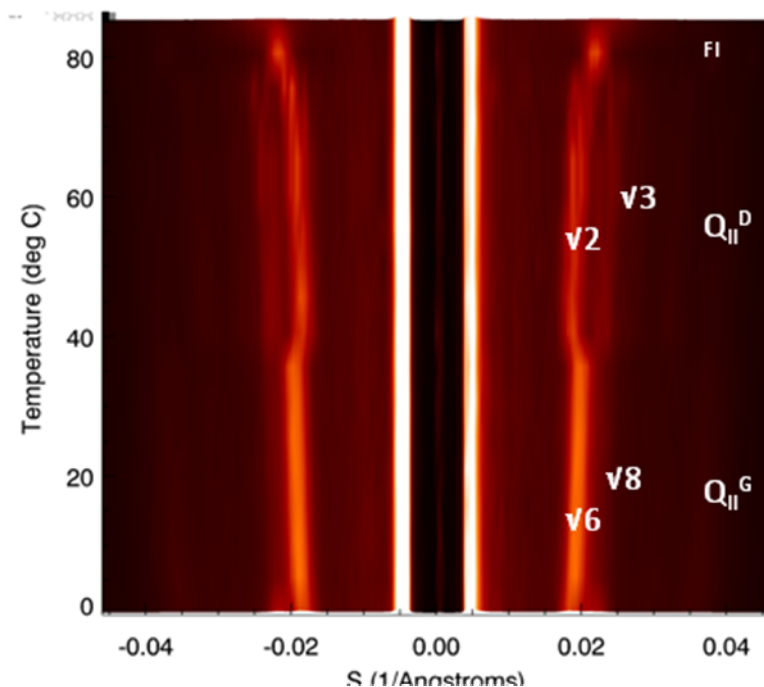


Figure S2c) Stack plot of equilibrium temperature scan from 0°C to 80°C in 5°C intervals for 25.1% wt water ML sample showing Q_{II}^G to Q_{II}^D to FI phase transition at 37.5°C and 75°C respectively.

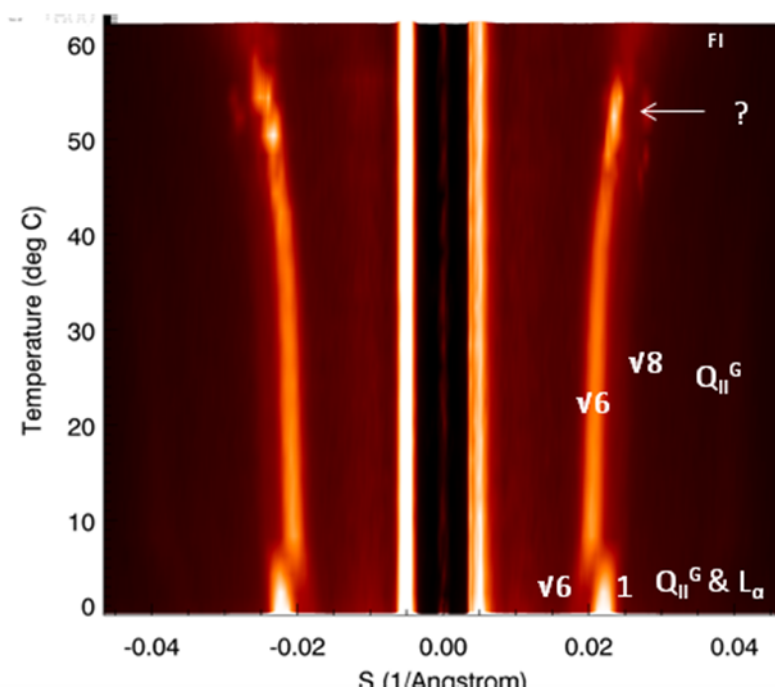


Figure S2d) Stack plot of equilibrium temperature scan from 0°C to 80°C in 2°C intervals for 22.8% wt water ML sample with lamellar and Q_{II}^G in coexistence from 0-6°C, pure Q_{II}^G phase from 6°C to 54°C and the Fluid Isotropic phase thereafter. An unidentified phase is seen prior to the transition to the FI phase

1. B. Gauthe, A. J. Heron, J. M. Seddon, O. Ces and R. H. Templer, *Rev. Sci. Instrum.*, 2009, **80**.
2. J. Seddon, A. Squires, C. Conn, O. Ces, A. Heron, X. Mulet, G. Shearman and R. Templer, *Philos. Trans. R. Soc. A*, 2006, **364**, 2635-2655.
3. Briggs and Caffrey, *J. Phys. II France*, 1996, **6**, 723-751.